

practice of referring to a molecule or an atom as ‘rehybridising’ is not good usage—the rehybridisation in question is in *our* picture, not in the molecule. It is likewise poor (but unfortunately common) practice to refer to atoms as being  $sp^3$ ,  $sp^2$  or  $sp$  hybridised. Again the atoms themselves are not, in a sense, hybridised, it is *we who have chosen to picture them that way*. It is better in such circumstances to refer to the atoms as being tetrahedral, trigonal, or digonal, as appropriate, and allow for the fact that the bonds around carbon (and other) atoms may not have exactly any of those geometries.

### 1.3.5 C—C $\sigma$ Bonds and $\pi$ Bonds: Ethane

With a total of fourteen valence electrons to accommodate in molecular orbitals, ethane presents a more complicated picture, and we now meet a C—C bond. We will not go into the full picture—finding the symmetry elements and identifying which atomic orbitals mix to set up the molecular orbitals. It is easy enough to see the various combinations of the 1s orbitals on the hydrogen atoms and the 2s, 2p<sub>x</sub>, 2p<sub>y</sub> and 2p<sub>z</sub> orbitals on the two carbon atoms giving the set of seven bonding molecular orbitals in Fig. 1.22.

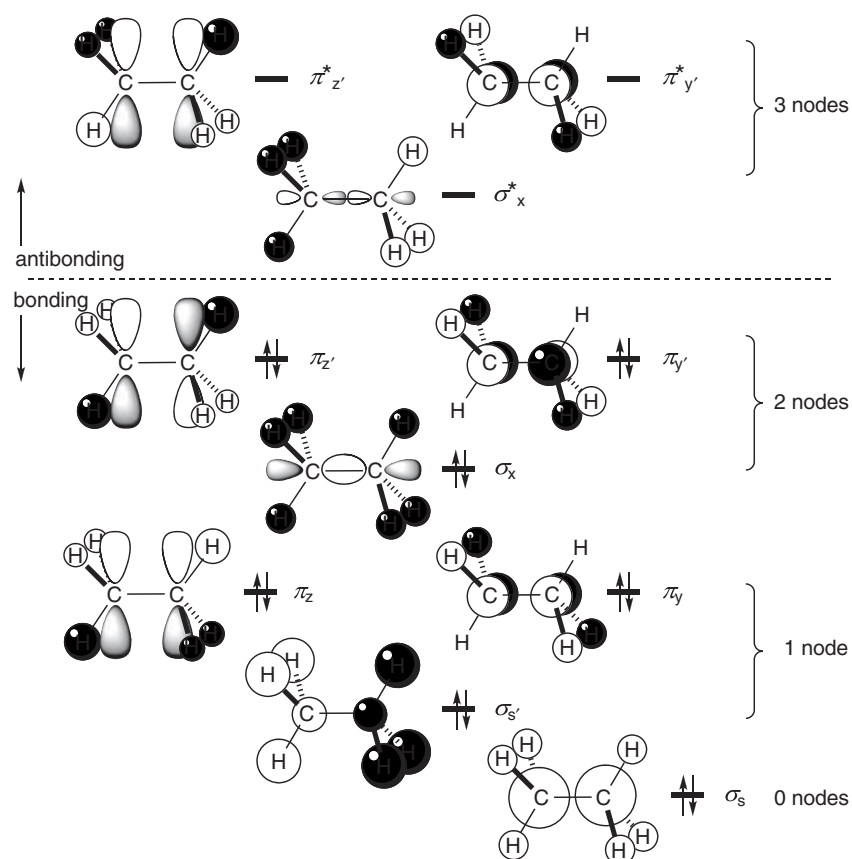


Fig. 1.22 The bonding orbitals and three antibonding orbitals of ethane

There is of course a corresponding picture using  $sp^3$  hybrids, but the following account shows how easy it is to avoid them. We shall concentrate for the moment on those orbitals which give rise to the force holding the two carbon atoms together; between them they make up the C—C bond. The molecular orbitals ( $\sigma_s$  and  $\sigma_{s'}$ ), made up

largely from 2s orbitals on carbon, are very like the orbitals in hydrogen, in that the region of overlap is directly on a line between the carbon nuclei; as before, they are called  $\sigma$  orbitals. The bonding in the lower one is very strong, but it is somewhat offset by the antibonding (as far as the C—C bond is concerned) in the upper one. They are both strongly bonding with respect to the C—H bonds. There is actually a little of the  $2p_x$  orbital mixed in with this orbital, just as we saw in Fig. 1.17 with a  $2p_z$  orbital, but most of the  $2p_x$  orbital contributes to the molecular orbital  $\sigma_x$ , which is also  $\sigma$  in character, and very strong as far as the C—C bond is concerned. This orbital has a little of the 2s orbital mixed in, resulting in the asymmetric extension of the lobes between the two carbon nuclei and a reduction in size of the outer lobes. This time, its antibonding counterpart ( $\sigma_x^*$ ) is not involved in the total bonding of ethane, nor is it bonding overall. It is in fact the lowest-energy antibonding orbital.

In the molecular orbitals using the  $2p_y$  and  $2p_z$  orbitals of carbon, the lobes of the atomic orbitals overlap sideways on. This is the distinctive feature of what is called  $\pi$  bonding, although it may be unfamiliar to meet this type of bonding in ethane. Nevertheless, let us see where it takes us. The conventional way of drawing a p orbital (Fig. 1.12c) is designed to give elegant and uncluttered drawings, like those in Fig. 1.22, and is used throughout this book for that reason. A better picture as we have already seen, and which we keep as a mental reservation when confronted with the conventional drawings, is the contour diagram (Fig. 1.12b). With these pictures in mind, the overlap sideways-on can be seen to lead to an enhanced electron population between the nuclei. However, since it is no longer directly on a line between the nuclei, it does not hold the carbon nuclei together as strongly as a  $\sigma$ -bonding orbital. The overlap integral  $S$  for two p orbitals with a dihedral angle of zero has the form shown in Fig. 1.23, where it can be compared with the corresponding  $\sigma$  overlap integral taken from Fig. 1.13b. Whereas the  $\sigma$  overlap integral goes through a maximum at about 1.5 Å and then falls rapidly to a value of  $-1$ , the  $\pi$  overlap integral rises more slowly but reaches unity at superimposition. Since C—C single bonds are typically about 1.54 Å long, the overlap integral at this distance for  $\pi$  bonding is a little less than half that for  $\sigma$  bonding.  $\pi$  Bonds are therefore much weaker.

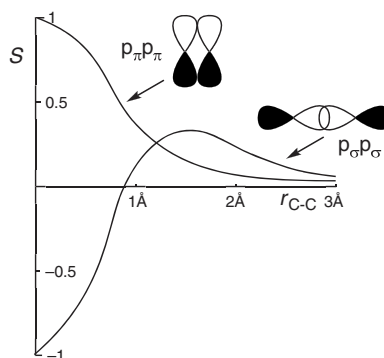


Fig. 1.23 Comparison of overlap integrals for  $\pi$  and  $\sigma$  bonding of p orbitals on C

Returning to the molecular orbitals in ethane made from the  $2p_y$  and  $2p_z$  orbitals, we see that they again fall in pairs, a bonding pair ( $\pi_y$  and  $\pi_z$ ) and (as far as C—C bonding is concerned, but not overall) an antibonding pair ( $\pi_y^*$  and  $\pi_z^*$ ). These orbitals have the wrong symmetry to have any of the 2s orbital mixed in with them. The electron population in the four orbitals ( $p_y$ ,  $p_z$ ,  $p_y^*$  and  $p_z^*$ ) is higher in the vicinity of the hydrogen atoms than in the vicinity of the carbon atoms, and these orbitals mainly contribute to the strength of the C—H bonds, towards which all four orbitals are bonding. The amount both of bonding and antibonding that they contribute to the C—C bond is small, with the bonding and antibonding combinations more or less cancelling each other out.

Thus the orbital ( $\sigma_x$ ) is the most important single orbital making up the C—C bond. We can construct for it an interaction diagram (Fig. 1.24), just as we did for the H—H bond in Fig. 1.3. The other major contribution to C—C bonding comes from the fact that  $\sigma_s$  is more C—C bonding than  $\sigma_s^*$  is C—C antibonding, as already mentioned.

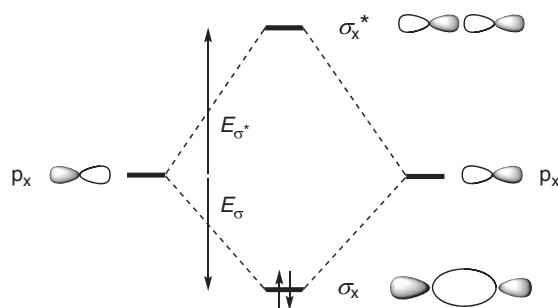


Fig. 1.24 A major part of the C—C  $\sigma$  bond of ethane

Had we used the concept of hybridisation, the C—C bond would, of course, simply have been seen as coming from the bonding overlap of  $sp^3$  hybridised orbitals on carbon with each other, and the overall picture for the C—C bond would have looked very similar to  $\sigma_x$  in Fig. 1.24, except that it would have used different proportions of s and p orbitals, and would have been labelled  $sp^3$ . For simplicity, we shall often discuss the orbitals of  $\sigma$  bonds as though they could be localised into bonding and antibonding orbitals like  $\sigma_x$  and  $\sigma_x^*$ . We shall not often need to refer to the full set of orbitals, except when they become important for one reason or another. Any property we may in future attribute to the bonding and antibonding orbitals of a  $\sigma$  bond, as though there were just one such pair, can always be found in the full set of all the bonding orbitals, or they can be found in the interaction of appropriately hybridised orbitals.

### 1.3.6 C=C $\pi$ Bonds: Ethylene

The orbitals of ethylene are made up from the 1s orbitals of the four hydrogen atoms and the 2s, 2p<sub>x</sub>, 2p<sub>y</sub> and 2p<sub>z</sub> orbitals of the two carbon atoms (Fig. 1.25). One group, made up from the 1s orbitals on hydrogen and the 2s, 2p<sub>x</sub> and 2p<sub>y</sub> orbitals on carbon, is substantially  $\sigma$  bonding, which causes the orbitals to be relatively low in energy. These five orbitals with ten of the electrons make up what we call the  $\sigma$  framework. Standing out, higher in energy than the  $\sigma$ -framework orbitals, is a filled orbital made up entirely from the 2p<sub>z</sub> orbitals of the carbon atom overlapping in a  $\pi$  bond. This time, the  $\pi$  orbital is localised on the carbon atoms with no mixing in of the 1s orbitals on the hydrogen atoms, which all sit in the nodal plane of the  $\pi_z$  orbital. The bonding in this orbital gives greater strength to the C—C bonding in ethylene than the  $\pi$  orbitals give to the C—C bonding in ethane, which is one reason why we talk of ethylene as having a *double* bond. Nevertheless, the C—C  $\sigma$  bonding in the  $\sigma$  framework is greater than the  $\pi$  bonding from overlap of the two p<sub>z</sub> orbitals. This is because, other things being equal,  $\pi$  overlap is inherently less effective in lowering the energy than  $\sigma$  overlap. Thus in the interaction diagram for a  $\pi$  bond (Fig. 1.26), the drop in energy  $E_\pi$  from  $\pi$  bonding is less than  $E_\sigma$  in Fig. 1.24 for comparable  $\sigma$  bonding, and this follows from the larger overlap integral for  $\sigma$  approach than for  $\pi$  approach (Fig. 1.23).

Similarly,  $E_{\pi^*}$  in Fig. 1.26 is less than  $E_{\sigma^*}$  in Fig. 1.24. Another consequence of having an orbital localised on two atoms is that the equation for the linear combination of atomic orbitals contains only two terms (Equation 1.1), and the  $c$ -values are again 0.707 in the bonding orbital and 0.707 and  $-0.707$  in the antibonding orbital. In simple Hückel theory, the energy of the p orbital on carbon is given the value  $\alpha$ , which is used as a reference point from which to measure rises and drops in energy, and will be especially useful when we come to deal with other elements. The value of  $E_\pi$  in Fig. 1.26 is given the symbol  $\beta$ , and is also used as a reference with which to compare the degree of bonding in other  $\pi$ -bonding systems. To give a sense of scale, its value for ethylene is approximately  $140 \text{ kJ mol}^{-1}$  ( $= 1.45 \text{ eV} = 33 \text{ kcal mol}^{-1}$ ). In other words the total  $\pi$  bonding in ethylene is  $280 \text{ kJ mol}^{-1}$ , since there are two electrons in the bonding orbital.

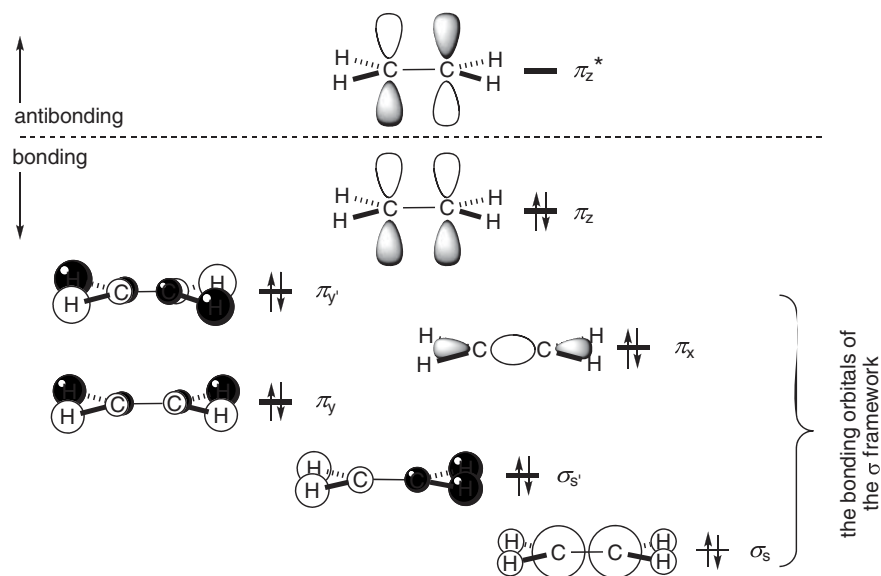


Fig. 1.25 The bonding orbitals and one antibonding orbital of ethylene

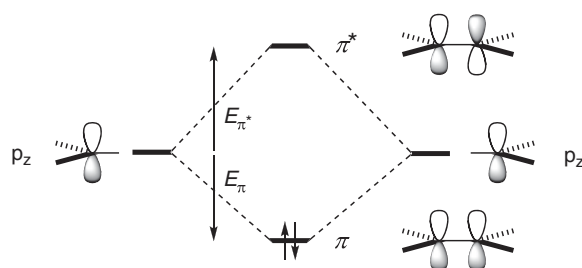
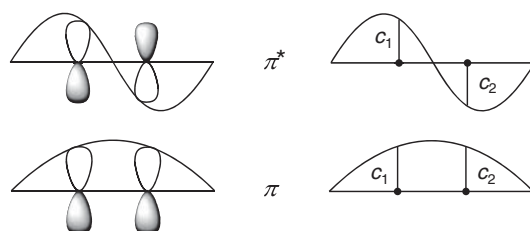


Fig. 1.26 A  $\text{C}=\text{C}$   $\pi$  bond

This separation of the  $\sigma$  framework and the  $\pi$  bond is the essence of Hückel theory. Because the  $\pi$  bond in ethylene in this treatment is self-contained, free of any complications from involvement with the hydrogen atoms, we may treat the electrons in it in the same way as we do for the fundamental quantum mechanical picture of an electron in a box. We look at each molecular wave function as one of a series of sine waves. In these simple molecules we only have the two energy levels, and so we only need to draw an analogy between them and the two lowest levels for the electron in the box. The convention is to draw the limits of the box *one bond length* out from the atoms at the end of the conjugated system, and then inscribe sine waves so that a node always comes at the edge of the box. With two orbitals to consider for the  $\pi$  bond of ethylene, we only need the  $180^\circ$  sine curve for  $\pi$  and the  $360^\circ$  sine curve for  $\pi^*$ . These curves can be inscribed over the orbitals as they are on the left of Fig. 1.27, and we can see on the right how the vertical lines above and below the atoms duplicate the pattern of the coefficients, with both  $c_1$  and  $c_2$  positive in the  $\pi$  orbital, and  $c_1$  positive and  $c_2$  negative in  $\pi^*$ .

The drawings of the  $p$  orbitals in Figs. 1.26 and 1.27 have the usual problem of being schematic. A better picture as we have already seen, and which we keep as a mental reservation when confronted with the



**Fig. 1.27** The  $\pi$  orbitals of ethylene and the electron in the box

conventional drawings, is the contour diagram (Fig. 1.12b). A better sense of the overlap from two side-by-side p orbitals is given in Fig. 1.28, where we see more clearly that in the bonding combination, even sideways-on, there is enhanced electron population between the nuclei, but that it is no longer directly on a line between the nuclei. The wire-mesh diagrams in Fig. 1.29, illustrate the shapes of the  $\pi$  and  $\pi^*$  orbitals even better, with some sense of their 3D character.

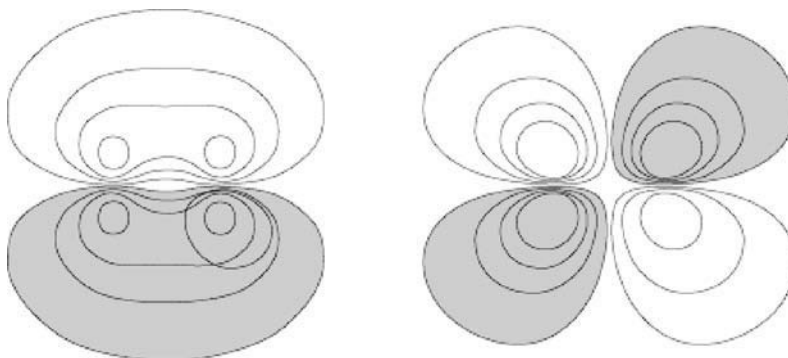


**Fig. 1.28** A section through the contours of the  $\pi$  and  $\pi^*$  wave functions of ethylene

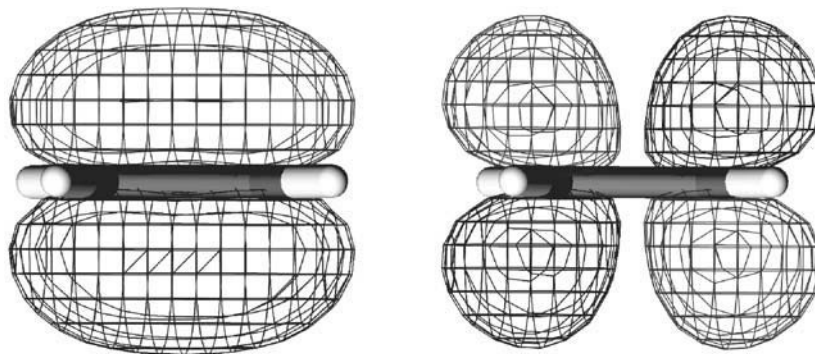


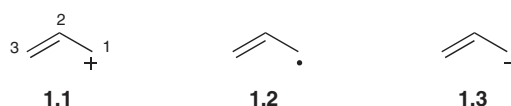
**Fig. 1.29** Wire-mesh outlines of one contour of the  $\pi$  and  $\pi^*$  wave functions of ethylene

## 1.4 Conjugation—Hückel Theory<sup>16,17</sup>

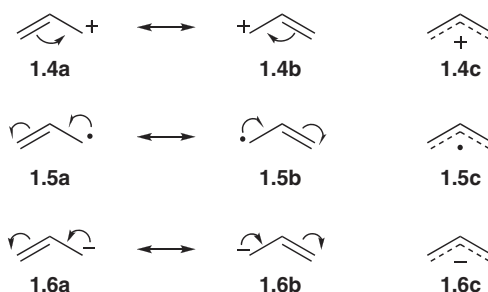
The interaction of atomic orbitals giving rise to molecular orbitals is the simplest type of conjugation. Thus in ethylene the two p orbitals can be described as being conjugated with each other to make the  $\pi$  bond. The simplest extension to make longer conjugated systems is to add one p orbital at a time to the  $\pi$  bond to make successively the  $\pi$  components of the allyl system with three carbon atoms, of butadiene with four, of the pentadienyl system with five, and so on. Hückel theory applies, because in each case we separate completely the  $\pi$  system from the  $\sigma$  framework, and we can continue to use the electron-in-the-box model.

### 1.4.1 The Allyl System

The members of the allyl system are reactive intermediates rather than stable molecules, and there are three of them: the allyl cation **1.1**, the allyl radical **1.2** and the allyl anion **1.3**. They have the same  $\sigma$  framework and the same  $\pi$  orbitals, but different numbers of electrons in the  $\pi$  system.

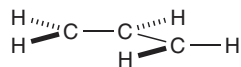


It is necessary to make a mental reservation about the diagrams **1.1–1.3**, so commonly used by organic chemists. These diagrams are localised structures that seem to imply that C-1 has the positive charge (an empty p orbital), the odd electron (a half-filled p orbital) or the negative charge (a filled p orbital), respectively, and that C-2 and C-3 are in a double bond in each case. However, we could have drawn the cation **1.1**, redrawn as **1.4a**, equally well the other way round as **1.4b**, and the curly arrow symbolism shows how the two *drawings* are interconvertible. This device is at the heart of valence bond theory. For now we need only to recognise that these two drawings are representations of the *same* species—there is no reaction connecting them, although many people sooner or later fall into the trap of thinking that ‘resonance’ like **1.4a**  $\rightarrow$  **1.4b** is a step in a reaction sequence. The double-headed arrow interconnecting them is a useful signal; this symbol should be used only for interconnecting ‘resonance structures’ and never to represent an equilibrium. There are corresponding pairs of drawings for the radical **1.5a** and **1.5b** and for the anion **1.6a** and **1.6b**.



One way of avoiding these misleading structures is to draw the allyl cation, radical or anion as in **1.4c**, **1.5c** and **1.6c**, respectively, illustrating the delocalisation of the p orbitals with a dashed line, and placing the positive or negative charge in the middle. The trouble with these drawings is that they are hard to use clearly with curly arrows in mechanistic schemes, and they do not show that the positive charge in the cation, the odd electron in the radical or the negative charge in the anion are largely concentrated on C-1 and C-3, the very feature that the drawings **1.4a** and **1.4b**, **1.5a** and **1.5b** and **1.6a** and **1.6b** illustrate so well. We shall see that the drawings with

apparently localised charges **1.4a**, **1.4b**, **1.5a** and **1.5b** and **1.6a** and **1.6b** illustrate not only the overall  $\pi$  electron distribution but also the important frontier orbital. It is probably better in most situations to use one of the localised drawings rather than any of the ‘molecular orbital’ versions **1.4c**, **1.5c** or **1.6c**, and then make the necessary mental reservation that each of the localised drawings implies the other.

**1.7**

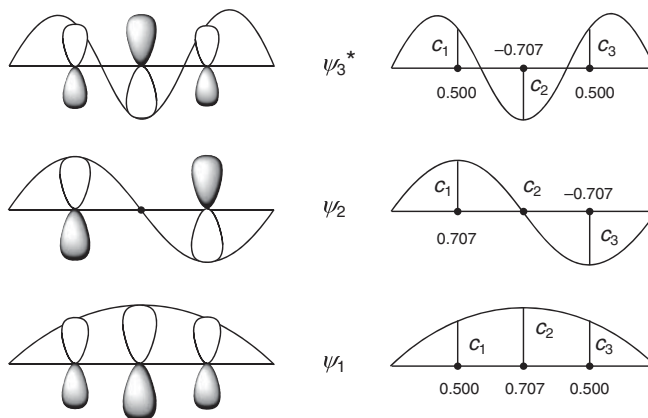
The allyl cation, radical and anion have the same  $\sigma$  framework **1.7**, with 14 bonding molecular orbitals filled with 28 electrons made by mixing the 1s orbitals of the five hydrogen atoms either with the  $sp^2$  hybrids or with the 2s, 2p<sub>x</sub> and 2p<sub>y</sub> orbitals of the three carbon atoms. The allyl systems are bent not linear, but we shall treat them as linear to simplify the discussion. The x, y and z coordinates have to be redefined as local x, y and z coordinates, different at each atom, in order to make this simplification, but this leads to no complications in the general story.

As with ethylene, we keep the  $\sigma$  framework separate from the  $\pi$  system, which is made up from the three p<sub>z</sub> orbitals on the carbon atoms that were not used in making the  $\sigma$  framework. The linear combination of these orbitals takes the form of Equation 1.9, with three terms, creating a pattern of three molecular orbitals,  $\psi_1$ ,  $\psi_2$  and  $\psi_3^*$ , that bear some resemblance to the set we saw in Section 1.3.3 for methylene. In the allyl cation there are two electrons left to go into the  $\pi$  system after filling the  $\sigma$  framework (and in the radical, three, and in the anion, four).

$$\psi = c_1\phi_1 + c_2\phi_2 + c_3\phi_3 \quad 1.9$$

We can derive a picture of these orbitals using the electron in the box, recognising that we now have three orbitals and therefore three energy levels. If the lowest energy orbital is, as usual, to have no nodes (except the inevitable one in the plane of the molecule), and the next one up one node, we now need an orbital with two nodes. We therefore construct a diagram like that of Fig. 1.27, but with one more turn of the sine curve, to include that for 540°, the next one up in energy that fulfils the criterion that there are nodes at the edges of the box, one bond length out, as well as the two inside (Fig. 1.30).

The lowest-energy orbital,  $\psi_1$ , has bonding across the whole conjugated system, with the electrons concentrated in the middle. Because of the bonding, this orbital will be lower in energy than an isolated p

**Fig. 1.30** The  $\pi$  orbitals of the allyl system



orbital. The next orbital up in energy  $\psi_2$ , is different from those we have met so far. Its symmetry demands that the node be in the middle; but this time the centre of the conjugated system is occupied by an *atom* and not by a *bond*. Having a node in the middle means having a zero coefficient  $c_2$  on C-2, and hence the coefficients on C-1 and C-3 in this orbital must be  $\pm 1/\sqrt{2}$ , if, squared and summed, they are to equal one. The atomic orbitals in  $\psi_2$  are so far apart in space that their repulsive interaction does not, to a first approximation, raise the energy of this molecular orbital relative to that of an isolated p orbital. In consequence, whether filled or not, it does not contribute to the overall bonding. If the sum of the squares of the three orbitals on C-2 is also to equal one, then the coefficients on C-2 in  $\psi_1$  and  $\psi_3^*$  must also be  $\pm 1/\sqrt{2}$ . Finally, since symmetry requires that the coefficients on C-1 and C-3 in  $\psi_1$  and  $\psi_3^*$  have the same absolute magnitude, and the sum of their squares must equal  $1 - (1/\sqrt{2})^2$ , we can deduce the unique set of  $c$ -values shown in Fig. 1.30. A pattern present in the allyl system because of its symmetry is seen with other symmetrical conjugated systems: the  $|c|$  values are reflected across a mirror plane placed horizontally, half way up the set of orbitals, between  $\psi_1$  and  $\psi_3^*$ , and also across a mirror plane placed vertically, through C-2. It is only necessary therefore to calculate four of the nine numbers in Fig. 1.30, and deduce the rest from the symmetry.

In this picture of the bonding, we get no immediate appreciation of the energies of these orbitals relative to those of ethylene. The nonbonding orbital  $\psi_2$  is clearly on the  $\alpha$  level, that of a p orbital on carbon, and  $\psi_1$  is lowered by the extra  $\pi$  bonding and  $\psi_3^*$  is raised. To assess the energies, there is a simple geometrical device that works for linear conjugated systems. The conjugated system, *including the dummy atoms at the ends of the sine curves*, is inscribed vertically inside a circle of radius  $2\beta$ , following the convention that one  $\pi$  bond in ethylene defines  $\beta$ . This is shown for ethylene and the allyl system in Fig. 1.31, where the dummy atoms are marked as dots at the top and bottom of the circle. The energies  $E$  of the  $\pi$  orbitals can then be calculated using Equation 1.10:

$$E = 2\beta \cos \frac{k\pi}{n+1} \quad 1.10$$

where  $k$  is the number of the atom along the sequence of  $n$  atoms. This is simply an expression based on the trigonometry of Fig. 1.31, where, for example, the  $\pi$  orbital of ethylene is placed on the first atom ( $k=1$ ) of the sequence of two ( $n=2$ ) reading anticlockwise from the bottom. Thus the energies of the  $\pi$  orbitals in the allyl system are  $1.414\beta$  below the  $\alpha$  level and  $1.414\beta$  above the  $\alpha$  level.

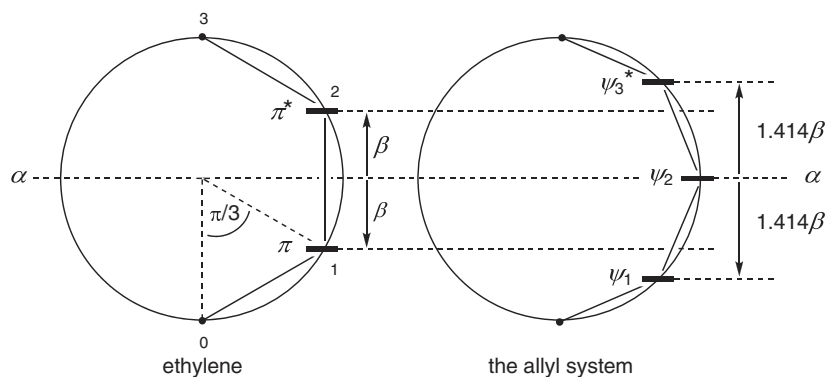
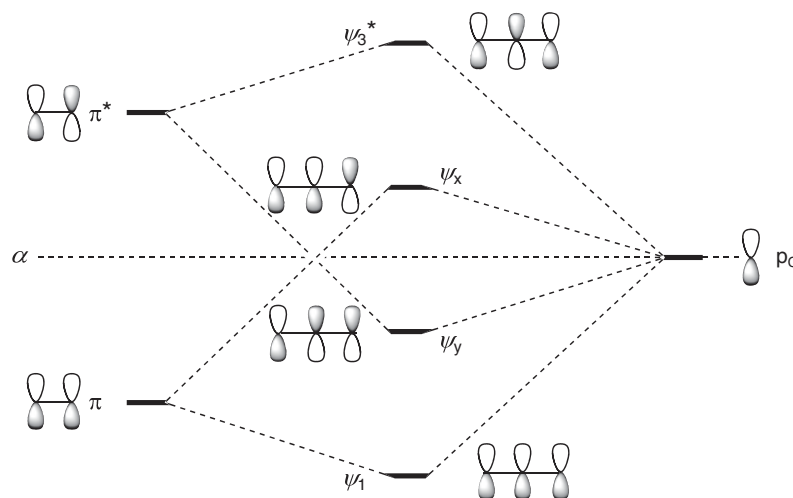


Fig. 1.31 Energies of  $\pi$  molecular orbitals in ethylene and the allyl system

We can gain further insight by building the picture of the  $\pi$  orbitals of the allyl system in another way. Instead of mixing together three p orbitals on carbon, we can combine two of them in a  $\pi$  bond first, as in Fig. 1.26, and then work out the consequences of having a third p orbital held within bonding distance of



the C=C  $\pi$  bond. Although Fig. 1.26, and all the interaction diagrams for single bonds, illustrated the bonding orbital as less bonding than the antibonding orbital is antibonding, this detail confuses the simple picture for conjugated systems that we want to build up here, and is left out of the discussion. We have to consider the effect of the p orbital, on the right of Fig. 1.32 on both the  $\pi$  and  $\pi^*$  orbitals of ethylene on the left. If we look *only* at the interaction with the  $\pi$  orbital, we can expect to create two new orbitals in much the same way as we saw when the two  $2p_z$  orbitals of carbon were allowed to interact in the formation of the  $\pi$  bond of Fig. 1.26. One orbital  $\psi_1$  will be lowered in energy and the other  $\psi_x$  raised. Similarly if we look *only* at its interaction with the  $\pi^*$  orbital, we can expect to create two new orbitals, one lowered in energy  $\psi_y$  and one raised  $\psi_3^*$ . We cannot create four orbitals from three, because we cannot use the p orbital separately twice.



**Fig. 1.32** A p orbital interacting independently with  $\pi$  and  $\pi^*$  orbitals. (No attempt is made to represent the relative sizes of the atomic orbitals)

We can see in Fig. 1.32 that the orbital  $\psi_1$  has been created by mixing the p orbital with the  $\pi$  orbital in a *bonding* sense, with the signs of the wave function of the two adjacent atomic orbitals matching. We can also see that the orbital  $\psi_3^*$  has been created by mixing the p orbital with the  $\pi^*$  orbital in an *antibonding* sense, with the signs of the wave functions unmatched. The third orbital that we are seeking,  $\psi_2$  in Fig. 1.33, is a combination created by mixing the p orbital with the  $\pi$  orbital in an *antibonding* sense *and* with the  $\pi^*$  orbital in a *bonding* sense. We do not get the two orbitals,  $\psi_x$  and  $\psi_y$  in Fig. 1.32, but something half way between, namely  $\psi_2$  in Fig. 1.33. By adding  $\psi_x$  and  $\psi_y$  in this way, the atomic orbitals drawn to the left of the energy levels labelled  $\psi_x$  and  $\psi_y$  in Fig. 1.32 cancel each other out on C-2 and reinforce each other on C-1 and C-3, thereby creating the molecular orbital  $\psi_2$  in Fig. 1.33.

We have of course arrived at the same picture for the molecular orbitals as that created from mixing the three separate p orbitals in Fig. 1.30. As before, the atomic orbitals in  $\psi_2$  are far enough apart in space for the molecular orbital  $\psi_2$  to have the same energy as the isolated p orbital in Fig. 1.33. It is a nonbonding molecular orbital (NBMO), as distinct from a bonding ( $\psi_1$ ) or an antibonding ( $\psi_3^*$ ) orbital. Again we see for the allyl cation, radical and anion, that, as a result of the overlap in  $\psi_1$ , the overall  $\pi$  energy of the allyl system has dropped relative to the sum of the energies of an isolated p orbital and of ethylene by  $2E$ , which we know from Fig. 1.31 is  $2 \times 0.414\beta$  or something of the order of  $116 \text{ kJ mol}^{-1}$  of extra  $\pi$  bonding relative to that in

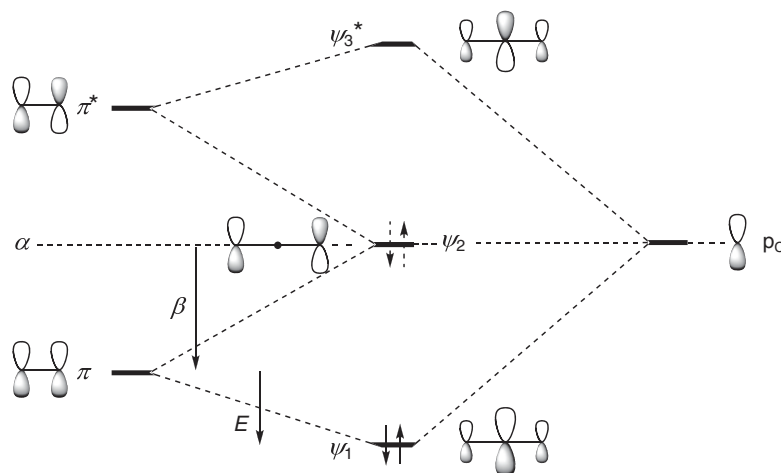


**Fig. 1.33** The allyl system by interaction of a p orbital with  $\pi$  and  $\pi^*$  orbitals

ethylene. In the radical and anion, where  $\psi_2$  has either one or two electrons, and  $\psi_3^*$  is still empty, the energy drop is still  $2E$ , because p and  $\psi_2$  are essentially on the same level. (It is not uncommon to express these drops in energy as a ‘gain’ in energy—in this sense, the gain is understood to be to us, or to the outside world, and hence means a loss of energy in the system and stronger bonding.)

It is worth considering at this stage what the overall  $\pi$  electron distribution will be in this conjugated system. The electron population in any molecular orbital is derived from the square of the atomic orbital functions, so that the sine waves describing the coefficients in Fig. 1.34a are squared to describe the electron distribution in Fig. 1.34b. The  $\pi$  electron population in the molecule as a whole is then obtained by adding up the electron populations, allowing for the number of electrons in each orbital, for all the *filled*  $\pi$  molecular orbitals. Looking only at the  $\pi$  system, we can see that the overall  $\pi$  electron distribution for the cation is

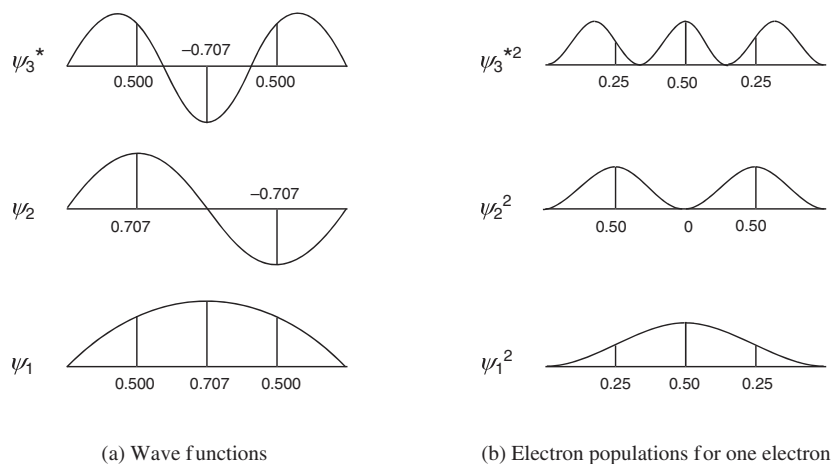


**Fig. 1.34** Wave functions and electron population for the allyl orbitals

derived from the squares of the coefficients in  $\psi_1$  alone, since this is the only populated  $\pi$  orbital. Roughly speaking, there is half an electron ( $2 \times 0.5^2$ ) on each of C-1 and C-3, and one electron ( $2 \times 0.707^2$ ) on C-2. This is illustrated graphically in Fig. 1.35a. Since the nucleus has a charge of +1, the excess charge on C-1 and C-3 is +0.5, in other words the electron deficiency in the cation is concentrated at the two ends.

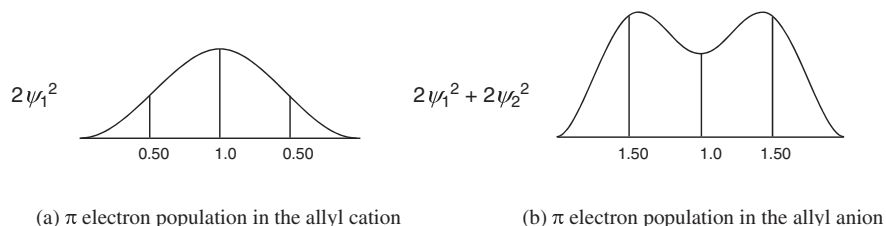


**Fig. 1.35** Total  $\pi$  electron populations in the allyl cation and anion

For the anion, the  $\pi$  electron population is derived by adding up the squares of the coefficients in both  $\psi_1$  and  $\psi_2$ . Since there are two electrons in both orbitals, there are 1.5 electrons ( $2 \times 0.5^2 + 2 \times 0.707^2$ ) roughly centred on each of C-1 and each of C-3, and one electron ( $2 \times 0.707^2$ ) centred on C-2. This is illustrated graphically in Fig. 1.35b. Subtracting the charge of the nucleus then gives the excess charge as  $-0.5$  on C-1 and C-3, in other words the electron excess in the anion is concentrated at the two ends. Thus the drawings of the allyl cation **1.4a** and **1.4b** illustrate the overall  $\pi$  electron population, and the corresponding drawings for the anion **1.6a** and **1.6b** do the same for that species.

As we shall see later, the most important orbitals with respect to reactivity are the highest occupied molecular orbital (HOMO) and the lowest unoccupied molecular orbital (LUMO). These are the *frontier orbitals*. For the allyl cation, the HOMO is  $\psi_1$ , and the LUMO is  $\psi_2$ . For the allyl anion, the HOMO is  $\psi_2$ , and the LUMO is  $\psi_3^*$ . The drawings of the allyl cation **1.4a** and **1.4b** emphasise not only the overall  $\pi$  electron population but even better emphasise the electron distribution in the LUMO. Similarly, the drawings of the allyl anion **1.6a** and **1.6b** emphasise the HOMO for that species. It is significant that it is the LUMO of the cation and the HOMO of the anion that will prove to be the more important frontier orbital in each case. In radicals, the most important orbital is the singly occupied molecular orbital (SOMO). For the allyl radical this is the half-filled orbital  $\psi_2$ . Once again, the drawings **1.5a** and **1.5b** emphasise the distribution of the odd electron in this orbital.

One final detail with respect to this, the most important orbital, is that it is not quite perfectly nonbonding. Although C-1 and C-3 are separated in space, they do interact slightly in  $\psi_2$ , as can be seen in the wire-mesh drawing of the nonlinear allyl system in Fig. 1.36, where the perspective allows one to see that the right hand

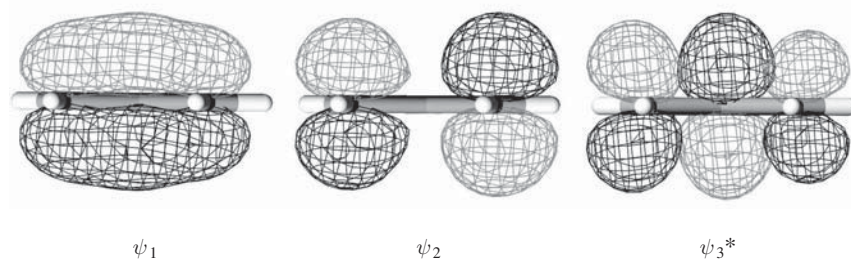
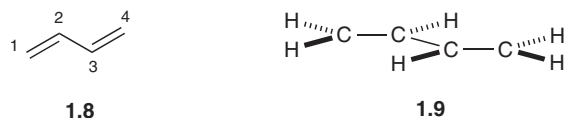


**Fig. 1.36** The  $\pi$  molecular orbitals of the allyl system

lobes, which are somewhat closer to the viewer, are just perceptibly repelled by the left hand lobes, and that neither of the atomic orbitals on C-1 and C-3 in  $\psi_2$  is a straightforwardly symmetrical p orbital. This orbital does not therefore have exactly the same energy as an isolated p orbital—it is slightly higher in energy.

### 1.4.2 Butadiene

The next step up in complexity comes with four p orbitals conjugated together, with butadiene **1.8** as the parent member. As usual there is a  $\sigma$  framework **1.9**, which can be constructed from the 1s orbitals of the six hydrogen atoms and either the  $sp^2$  hybrids of the four carbon atoms or the separate 2s,  $2p_x$  and  $2p_y$  orbitals. The  $\sigma$  framework has 18 bonding molecular orbitals filled with 36 electrons. Again we have two ways by which we may deduce the electron distribution in the  $\pi$  system, made up from the four  $p_z$  orbitals and holding the remaining four electrons. Starting with the electron in the box with four p orbitals, we can construct Fig. 1.37, which shows the four wave functions, inside which the p orbitals are placed at the appropriate regular intervals.



We get a new set of orbitals,  $\psi_1$ ,  $\psi_2$ ,  $\psi_3^*$ , and  $\psi_4^*$ , each described by Equation 1.11 with four terms:

$$\psi = c_1\phi_1 + c_2\phi_2 + c_3\phi_3 + c_4\phi_4 \quad 1.11$$

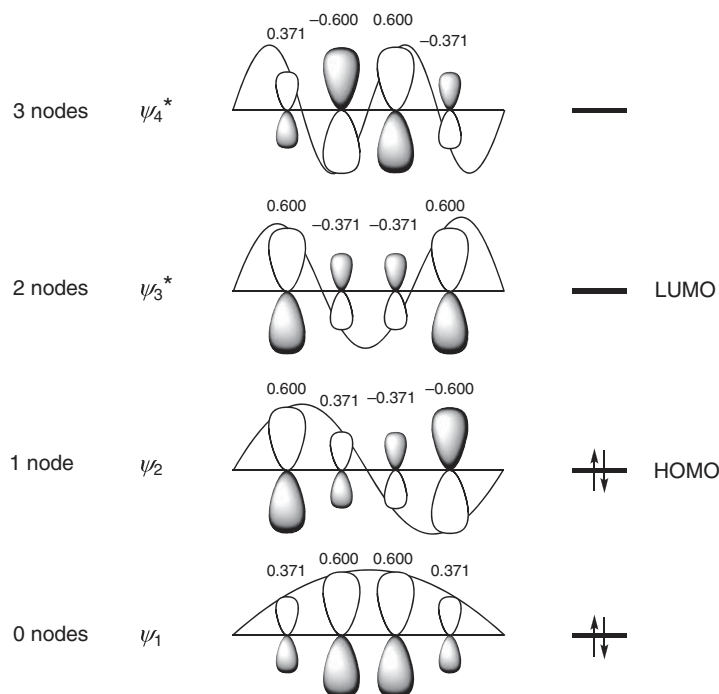


**Fig. 1.37**  $\pi$  Molecular orbitals of butadiene

The lowest-energy orbital  $\psi_1$  has all the  $c$ -values positive, and hence bonding is at its best. The next-highest energy level has one node, between C-2 and C-3; in other words,  $c_1$  and  $c_2$  are positive and  $c_3$  and  $c_4$  are negative. There is therefore bonding between C-1 and C-2 and between C-3 and C-4, but not between C-2 and C-3. With two bonding and one antibonding interaction, this orbital is also overall bonding. Thus the lowest-energy orbital of butadiene,  $\psi_1$ , reasonably enough, has a high population of electrons in the middle, but in the next orbital up,  $\psi_2$ , because of the repulsion between the wave functions of opposite sign on C-2 and C-3, the electron population is concentrated at the ends of the conjugated system. Overall, summing the squares of the coefficients of the filled orbitals,  $\psi_1$  and  $\psi_2$ , the  $\pi$  electrons are, at this level of approximation, evenly spread over all four carbon atoms of the conjugated system.

We can easily give numerical values to these coefficients, using the convention that the edge of the box is drawn one bond length out from the terminal carbon atoms. Treating the conjugated system as being linear, the coefficients are proportional to the sine of the angle, as defined by the position of the atom within the sine curve. The algebraic expression for this idea in the general case, and illustrated in Fig. 1.37 for the specific case of butadiene, with the atomic orbitals inscribed within the sine curves, is Equation 1.12:

$$c_{jr} = \sqrt{\frac{2}{n+1}} \sin \frac{rj\pi}{n+1} \quad 1.12$$

giving the coefficient  $c_{jr}$  for atom  $j$  in molecular orbital  $r$  of a conjugated system of  $n$  atoms (so that  $j$  and  $r = 1, 2, 3, \dots, n$ ). The expression in front of the sine function is the normalisation factor to make the squares of the coefficients add up to one. Thus, taking  $\psi_2$  for butadiene ( $r = 2$ ,  $n = 4$  and the sine curve is a full  $2\pi$ ): the normalisation factor for  $n = 4$  is 0.632, the angle for the first atom ( $j = 1$ ) is  $2\pi/5$ , the sine of which is 0.951, and the coefficient  $c_1$  is the product  $0.632 \times 0.951 = 0.600$ . Similarly,  $c_2$  is 0.371,  $c_3$  is  $-0.371$  and  $c_4$  is  $-0.600$ .

Large lists of coefficients for conjugated systems, some as easily calculated as butadiene above, some more complicated, have been published.<sup>18</sup> As with the allyl system, other patterns are also present because of the symmetry of the molecule: for alternant conjugated systems (those having no odd-membered rings), the  $|c|$  values are reflected across a mirror plane placed horizontally, half way between  $\psi_2$  and  $\psi_3^*$ , and also across a mirror plane placed vertically, half way between C-2 and C-3. It is only necessary therefore to calculate four of the 16 numbers in Fig. 1.37, and deduce the rest from the symmetry.

Alternatively, we can set up the conjugated system of butadiene by looking at the consequences of allowing two isolated  $\pi$  bonds to interact, as they will if they are held within bonding distance. It is perhaps a little easier to see on this diagram the pattern of raised and lowered energy levels relative to those of the  $\pi$  bonds from which they are derived. Let us first look at the consequence of allowing the orbitals close in energy to interact, which they will do strongly (Fig. 1.38). (For a brief account of how the energy difference between interacting orbitals affects the extent of their interaction, see the discussion of Equations 1.13 and 1.14 on p. 54.) The interactions of  $\pi$  with  $\pi$  and of  $\pi^*$  with  $\pi^*$  on the left create a new set of orbitals,  $\psi_a$ - $\psi_d^*$ . This is not the whole story, because we must also allow for the weaker interaction, shown on the right, of the orbitals further apart in energy,  $\pi$  with  $\pi^*$ , which on their own would create another set of orbitals,  $\psi_w$ - $\psi_z^*$ .

Mixing these two sets together, and allowing for the greater contribution from the stronger interactions, we get the set of orbitals (Fig. 1.39), matching those we saw in Fig. 1.37. Thus, to take just the filled orbitals, we see that  $\psi_1$  is derived by the interaction of  $\pi$  with  $\pi$  in a bonding sense ( $\psi_a$ ), lowering the energy of  $\psi_1$  below that of the  $\pi$  orbital, and by the interaction of  $\pi$  with  $\pi^*$  in a bonding sense ( $\psi_w$ ), also lowering the energy below that of the  $\pi$  orbital. Since the former is a strong interaction and the latter weak, the net effect is to lower the energy of  $\psi_1$  below the  $\pi$  level, but by a little more than the amount ( $\beta$  in simple Hückel theory, illustrated as  $E_\pi$  in Fig. 1.26) that a  $\pi$  orbital is lowered below the p level (the dashed line  $\alpha$  in Figs. 1.31, 1.32 and 1.33, called  $\alpha$  in simple Hückel theory) in making the  $\pi$  bond of ethylene. However,  $\psi_2$  is derived from the interaction of  $\pi$  with  $\pi$  in an antibonding sense ( $\psi_b$ ), raising the energy above that of the  $\pi$  orbital, and by the interaction of  $\pi^*$  with  $\pi$  in a bonding sense ( $\psi_x$ ), lowering it again. Since the former is a strong interaction

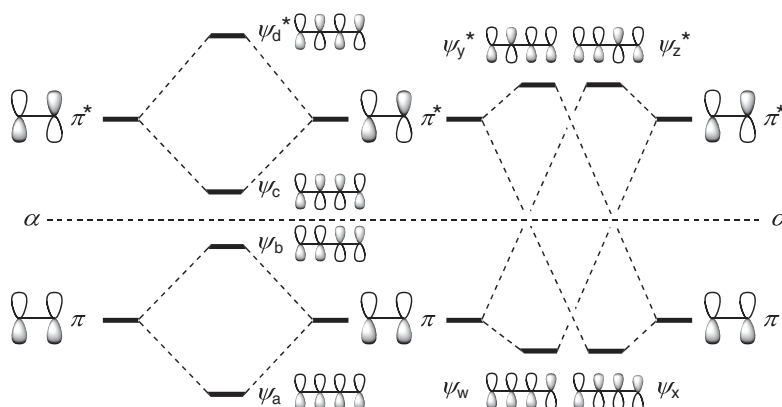


**Fig. 1.38** Primary interactions of the  $\pi$  molecular orbitals of two molecules of ethylene. (No attempt is made to represent the relative sizes of the atomic orbitals)

and the latter weak, the net effect is to raise the energy of  $\psi_2$  above the  $\pi$  level, but not by as much as a  $\pi^*$  orbital is raised above the p level in making the  $\pi$  bond of ethylene. Yet another way of looking at this system is to say that the orbitals  $\psi_1$  and  $\psi_2$  and the orbitals  $\psi_3^*$  and  $\psi_4^*$  mutually repel each other.

We are now in a position to explain the well-known property that conjugated systems are often, but not always, lower in energy than unconjugated systems. It comes about because  $\psi_1$  is lowered in energy more than  $\psi_2$  is raised ( $E_1$  in Fig. 1.39 is larger than  $E_2$ ). The energy ( $E_1$ ) given out in forming  $\psi_1$  comes from the

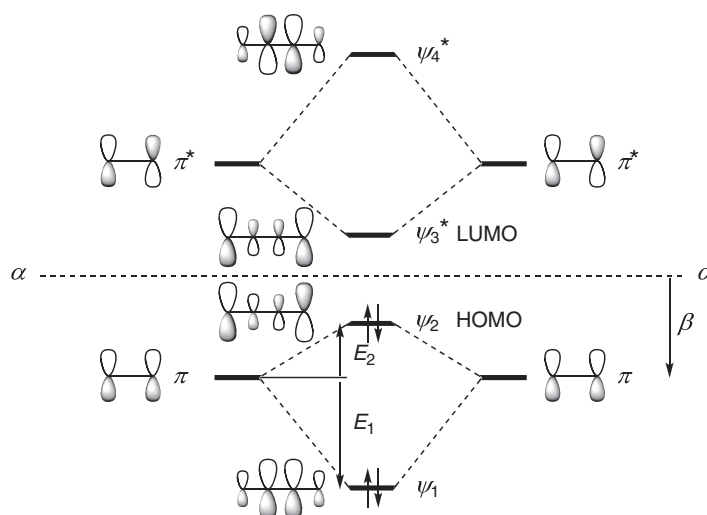


**Fig. 1.39** Energies of the  $\pi$  molecular orbitals of ethylene and butadiene by orbital interaction

overlap between the atomic orbitals on C-2 and C-3; this overlap did not exist in the isolated  $\pi$  bonds. It is particularly effective in lowering the energy of  $\psi_1$ , because the coefficients on C-2 and C-3 are large. By contrast, the increase in energy of  $\psi_2$ , caused by the repulsion between the orbitals on C-2 and C-3, is not as great, because the coefficients on these atoms are smaller in  $\psi_2$ . Thus the energy lost from the system in forming  $\psi_1$  is greater than the energy needed to form  $\psi_2$ , and the overall  $\pi$  energy of the ground state of the system ( $\psi_1^2\psi_2^2$ ) is lower. We can of course see the same pattern, and attach some very approximate numbers, using the geometrical analogy. This is illustrated in Fig. 1.40, which shows that  $\psi_2$  is raised above  $\pi$  by  $0.382\beta$  and  $\psi_1$  is lowered below  $\pi$  by  $0.618\beta$ . The overall lowering in energy for the extra conjugation is therefore  $(2 \times 0.618 + 2 \times 1.618) - 4 = 0.472\beta$  or about  $66 \text{ kJ mol}^{-1}$ .

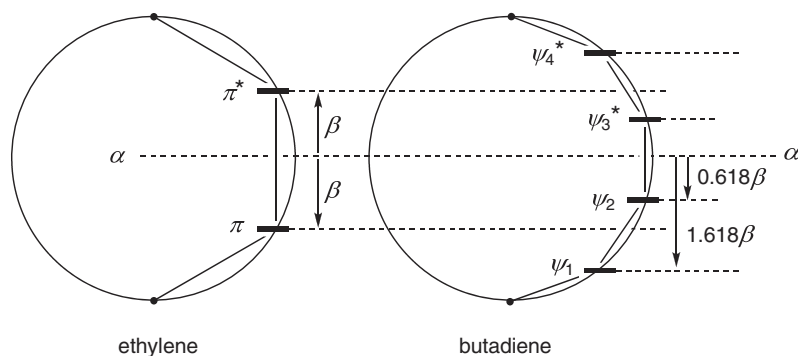


Fig. 1.40 Energies of the  $\pi$  molecular orbitals of ethylene and butadiene by geometry

Before we leave butadiene, it is instructive to look at the same  $\pi$  orbitals in wire-mesh diagrams (Fig. 1.41) to reveal more accurately what the electron distribution in the  $\pi$  molecular orbitals looks like. In the allyl system and in butadiene, we have seen more than one filled and more than one empty orbital in the same molecule. The  $\sigma$  framework, of course, with its strong  $\sigma$  bonds, has several other filled orbitals lying lower in energy than either  $\psi_1$  or  $\psi_2$ , but we do not usually pay much attention to them when we are thinking of reactivity, simply because they lie so much lower in energy. In fact, we shall be paying special attention to the filled molecular orbital which is highest in energy ( $\psi_2$ , the HOMO) and to the unoccupied orbital of lowest energy ( $\psi_3^*$ , the LUMO).

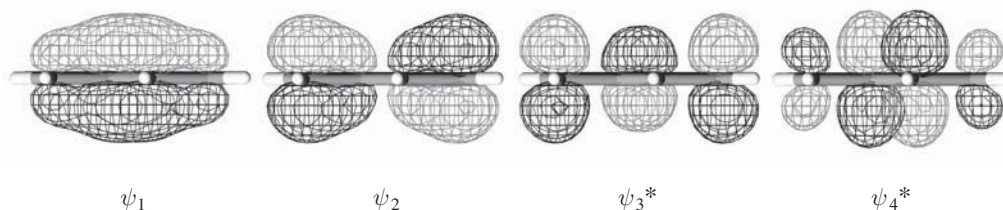
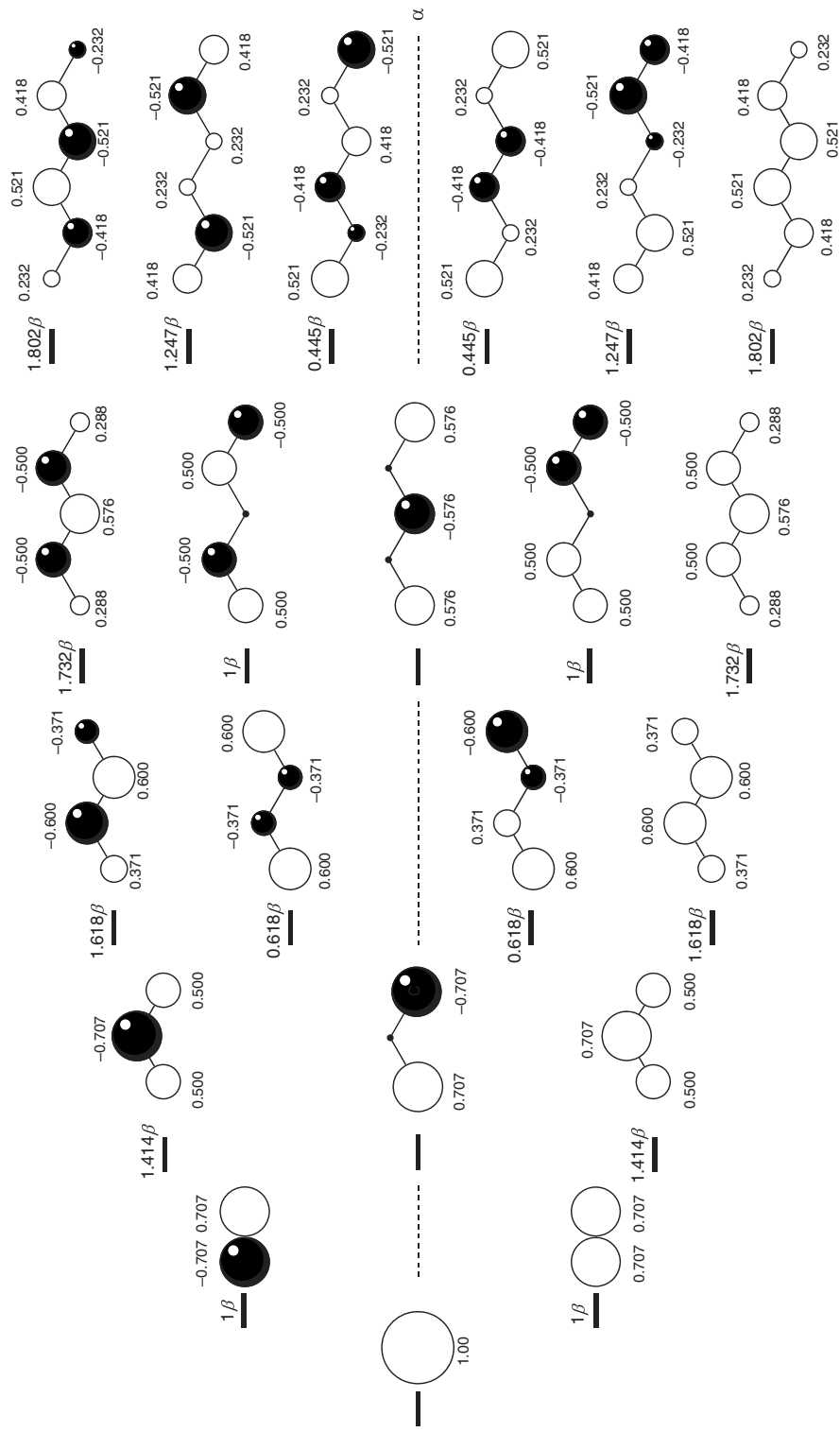


Fig. 1.41 The  $\pi$  molecular orbitals of butadiene in the *s-trans* conformation

### 1.4.3 Longer Conjugated Systems

In extending our understanding to the longer linear conjugated systems, we need not go through all the arguments again. The methods are essentially the same. The energies and coefficients of the  $\pi$  molecular orbitals for all six systems from an isolated p orbital up to hexatriene are summarised in Fig. 1.42. The viewpoint in this drawing is directly above the p orbitals, which appear therefore to be circular. This is a common simplification, rarely likely to lead to confusion between a p orbital and an s orbital, and we shall use it through much of this book.





**Fig. 1.42** The energies and coefficients of the  $\pi$  molecular orbitals of the smaller conjugated systems

The longer the conjugated system, the lower the energy of  $\psi_1$ , but each successive drop in energy is less than it was for the system with one fewer atoms, with a limit at infinite length of  $2\beta$ . Among the even-atom species, the longer the conjugated system, the higher the energy of the HOMO, and the lower the energy of the LUMO, with the energy gap becoming ever smaller. With a narrow HOMO–LUMO gap, polyenes allow the easy promotion of an electron from the HOMO to the LUMO, and the longer the conjugated system, the easier it is, making the absorption of UV and visible light ever less energetic. Most organic chemists will be happy with this picture, and most of the consequences in organic chemistry can be left at this level of understanding.

At the extreme of an infinite polyene, however, simple Hückel theory reduces the HOMO–LUMO gap to zero, since the secants in diagrams like Fig. 1.40, would become infinitely small as they moved to the perimeter of the circle. Such a polyene would have equal bond lengths between each pair of carbon atoms, there would be no gap between the HOMO and the LUMO, and it would be a metallic conductor. This is not what happens—long polyenes, like polyacetylene, have alternating double (or triple) and single bonds, and their interconversion, which is the equivalent of the movement of current along the chain, requires energy. The theoretical description of this modification to simple Hückel theory is known by physicists as a Peierls distortion. It has its counterpart for chemists in the Jahn-Teller distortion seen, for example, in cyclobutadiene, which distorts to have alternating double and single bonds, avoiding the degenerate orbitals and equal bond lengths of square cyclobutadiene (see Section 1.5.2). The simple Hückel picture is evidently wrong at this extreme of very long conjugated systems. One way of appreciating what is happening is to think of the HOMO and the LUMO interacting more strongly when they are close in energy, just as the filled and unfilled orbitals of butadiene repel each other (Fig. 1.39), but more so. The residual gap, corresponding approximately to what is called by physicists the ‘band-gap energy’, is amenable to tuning, by attaching suitable substituents, just like any other HOMO–LUMO gap. Tailoring it has proved to be a basis for tuning the properties of optical devices.<sup>19</sup>

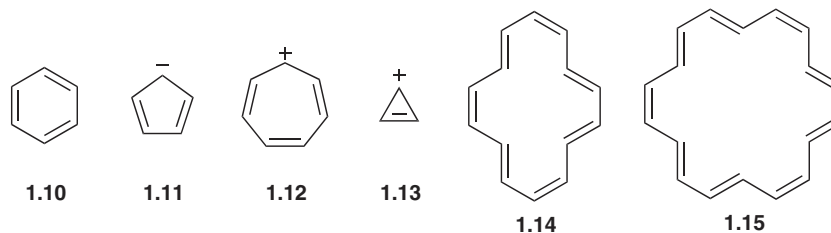
The process by which alternating double and single bonds might exchange places is strictly forbidden by symmetry, but occurs in practice, because the mismatch in symmetry of adjacent elements is disrupted by having an atom lacking an electron or carrying an extra electron in the chain.<sup>20</sup> Thus an ‘infinite’ polyene can have long stretches of alternating single and double bonds interrupted by a length of conjugated p orbitals resembling a conjugated cation, radical or anion. Such ‘defects’ are chains of conjugated atoms, but like the chain of the polyene itself, the feature of equal bond lengths does not stretch infinitely along the whole ‘molecule’, as simple Hückel theory would suggest. It is limited in what physicists call ‘solitons’. In the soliton, there is no bond alternation at its centre, but bond alternation appears at greater distances out from its centre. Solitons provide a mechanism for electrical conduction along the chain, which is described as being ‘doped’. Unfortunately, the physicists’ nomenclature in the polymer area departs from that of the organic chemist, with expressions like ‘tight binding model’ meaning much the same as the LCAO approximation, ‘band structure’ for the stack of orbitals, ‘band gap’ for the HOMO–LUMO gap, ‘valence band’ for the HOMO, ‘Fermi energy’ meaning roughly the same as the energy of the HOMO, and the ‘conduction band’ meaning roughly the same as the LUMO. The physical events are of course similar, and the comparisons have been elegantly discussed.<sup>21</sup> Such a breakdown in Hückel theory is not normally encountered in organic chemistry, where delocalisation can be expected to stretch undeterred by the length of the conjugated systems in what we might call ordinary molecules.

## 1.5 Aromaticity<sup>22</sup>

### 1.5.1 Aromatic Systems

One of the most striking properties of conjugated organic molecules is the special stability found in the group of molecules called aromatic, with benzene **1.10** as the parent member and the longest established example. Hückel predicted that benzene was by no means alone, and that cyclic conjugated polyenes would have exceptionally low energy if the total number of  $\pi$  electrons could be described as a number of the form  $(4n + 2)$ , where  $n$  is an integer. Other  $6\pi$ -electron cyclic systems such as the cyclopentadienyl anion **1.11** and the cycloheptatrienyl cation **1.12** belong in this category. The cyclopropenyl cation **1.13** ( $n = 0$ ),

[14]annulene **1.14** ( $n=3$ ), [18]annulene **1.15** ( $n=4$ ) and many other systems have been added over the years.<sup>23</sup> Where does this special stability come from?



We can approach this question in much the same way as we approached the derivation of the molecular orbitals of conjugated systems. We begin with a  $\sigma$  framework containing the C—C and C—H  $\sigma$  bonds. We must then deduce the nodal properties of the  $\pi$  molecular orbitals created from six p orbitals in a ring. They are all shown both in elevation and in plan in Fig. 1.43. The lowest-energy orbital  $\psi_1$  has no node as usual, but because the conjugated system goes round the ring instead of spilling out at the ends of the molecule, as it did

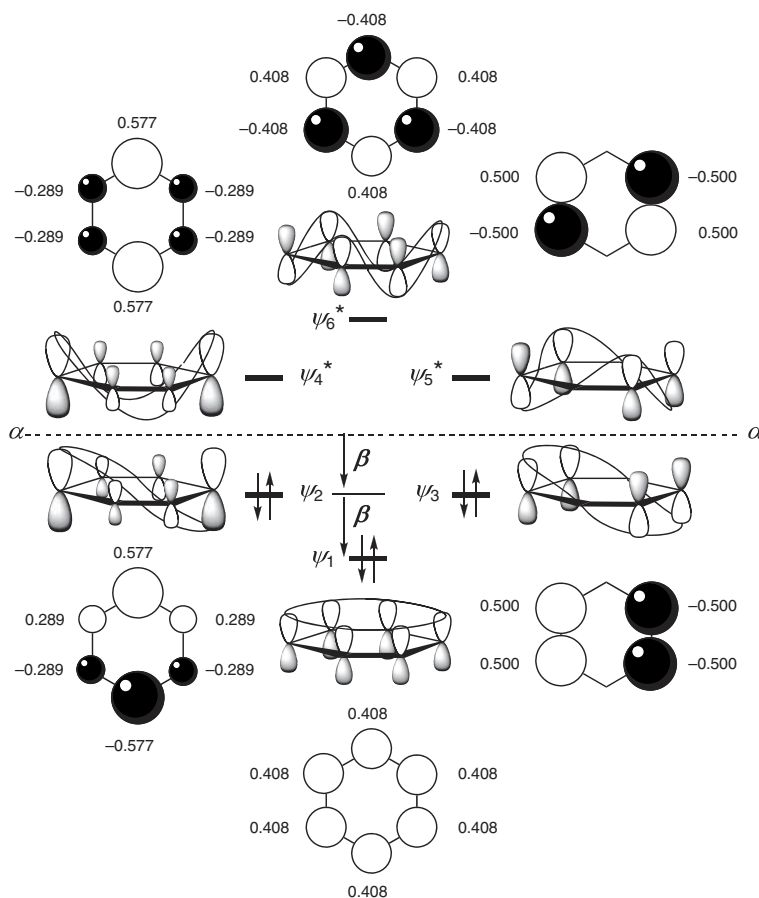


Fig. 1.43 The  $\pi$  molecular orbitals of benzene

with the linear conjugated systems, the coefficients on all six atoms are equal. The other special feature is that there are two orbitals having the same energy with one node  $\psi_2$  and  $\psi_3$ , because they can be created in two symmetrical ways, one with the node horizontal  $\psi_2$  and one with it vertical  $\psi_3$ . Similarly, there are two orbitals,  $\psi_4^*$  and  $\psi_5^*$ , with the same energy having two nodes. Finally there is the one orbital,  $\psi_6^*$ , with three nodes.

The size of the coefficients can be deduced from the position of the atoms within the sine curves, in the usual way. They support the assumption from symmetry that the amount of bonding in  $\psi_2$  equals that in  $\psi_3$ . Thus the allyl-like overlap in the two halves of  $\psi_2$  has bonding between a large ( $\pm 0.577$ ) and two small ( $\pm 0.289$ ) lobes, whereas the antibonding interaction is between the two small lobes. The result is actually a lowering of energy for this orbital equal to that of the  $\pi$  bond in ethylene ( $\beta$ ). In  $\psi_3$  there is bonding between lobes of intermediate size ( $\pm 0.500$ ) and the interaction across the ring between the lobes of opposite sign is, like  $\psi_2$  in the allyl system, nonbonding rather than antibonding. Overlap between the p orbitals in ethylene ( $c = 0.707$ ) gives rise to a lowering of energy ( $\beta$ ) worth one full  $\pi$  bond. Overlap between two lobes of the same sign in  $\psi_3$  with coefficients of  $\pm 0.50$  gives rise to half a  $\pi$  bond ( $0.707^2 = 0.500$ ), and two such interactions comes again to one full  $\pi$  bond. The fully bonding overlap of the six orbitals ( $c = 0.408$ ) in  $\psi_1$  gives rise to two  $\pi$  bond's worth of bonding. The total of  $\pi$  bonding is thus  $2 \times 4\beta$ , which is two more  $\beta$  units than three *isolated*  $\pi$  bonds. Benzene is also lowered in  $\pi$  energy by more than the amount for three *linearly conjugated*  $\pi$  bonds: taking the numbers for hexatriene from Fig. 1.40, the total of  $\pi$  bonding is  $2 \times (1.802 + 1.247 + 0.445)\beta = 7\beta$ . The extra  $\pi$  bonding is the special feature of aromatic systems.

The energies of the molecular orbitals can also be deduced by the same device, used for linear conjugated systems, of inscribing the conjugated system inside a circle of radius  $2\beta$ . There is no need for dummy atoms, since the sine curves go right round the ring, and the picture is therefore that shown in Fig. 1.44.

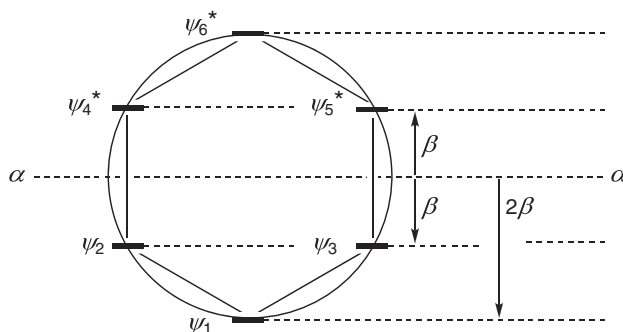
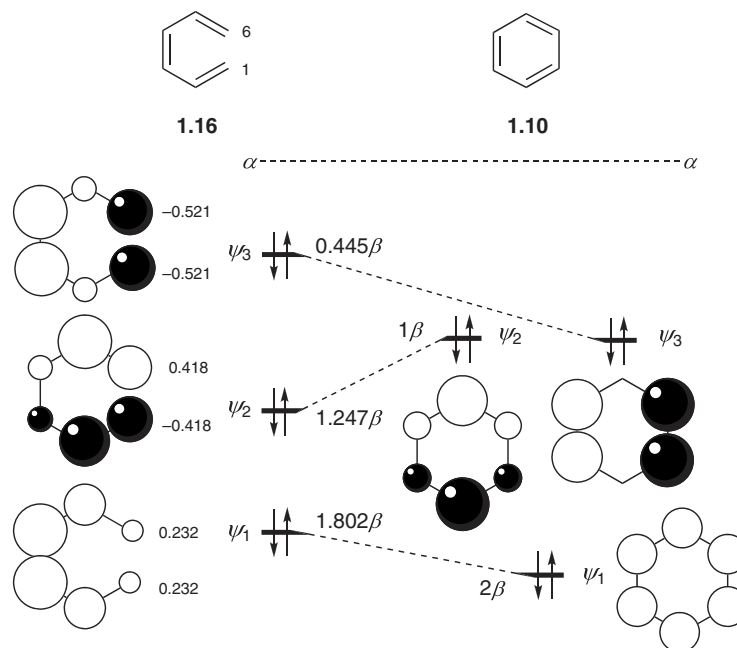


Fig. 1.44 The energies of the  $\pi$  molecular orbitals of benzene

It is also possible to find the source of aromatic stabilisation by looking at an interaction diagram. For benzene **1.10**, one way is to start with hexatriene **1.16**, and examine the effect of bringing the ends of the conjugated system, C-1 and C-6, within bonding distance (Fig. 1.45). Since we are only looking at the  $\pi$  energy, we ignore the C—H bonds, and the fact that to carry out this ‘reaction’ we would have to break two of them and make a C—C  $\sigma$  bond in their place. In  $\psi_1$  and  $\psi_3$  the atomic orbitals on C-1 and C-6 have the same sign on the top surface. Bringing them within bonding distance will increase the amount of  $\pi$  bonding, and lower the energy of  $\psi_1$  and  $\psi_3$  in going from hexatriene to benzene. In  $\psi_2$  however, the signs of the atomic orbitals on C-1 and C-6 are opposite to each other on the top surface, and bringing them within bonding distance will be antibonding, raising the energy of  $\psi_2$  in going from hexatriene to benzene. The overall result is two drops in energy to one rise, and hence a lowering of  $\pi$  energy overall.



**Fig. 1.45** The drop in  $\pi$  energy in going from hexatriene to benzene

However, the ups and downs are not all equal as Fig. 1.45, which is drawn to scale, shows. The net lowering in  $\pi$  energy, relative to hexatriene, is actually only one  $\beta$  value, as we deduced above, not two. It is barely legitimate, but there is some accounting for this difference—the overlap raising the energy of  $\psi_2$  and lowering the energy of  $\psi_3$  is between orbitals with large coefficients, more or less cancelling one another out; however, the overlap between C-1 and C-6 in  $\psi_1$  is between orbitals with a small coefficient, making that drop close to  $0.5\beta$  as shown in Fig. 1.45.

One of the most striking artifacts of aromaticity, in addition to the lowering in energy, is the diamagnetic anisotropy, which is characteristic of these rings. Although known long before NMR spectroscopy was introduced into organic chemistry, its most obvious manifestation is in the downfield shift experienced by protons on aromatic rings, and perhaps even more vividly by the upfield shift of protons on the inside of the large aromatic annulenes. The theory<sup>24,25</sup> is beyond the scope of this book, but it is associated with the system of  $\pi$  molecular orbitals, and can perhaps be most simply appreciated from the idea that the movement of electrons round aromatic rings is free, like that in a conducting wire, as epitomised by the equal C—C bond lengths.

Like the conjugation in polyenes that we saw earlier, aromaticity does not stretch to infinitely conjugated cyclic systems, even when they do have  $(4n+2)$  electrons. Just as long polyenes do not approach a state with equal bond lengths as the number of conjugated double bonds increases, the  $(4n+2)$  rule of aromaticity breaks down, with bond alternation setting in when  $n$  reaches a large number. It is not yet clear what that number is with neither theory nor experiment having proved decisive. Early predictions<sup>26</sup> that the largest possible aromatic system would be [22] or [26]annulene were too pessimistic, and aromaticity, using the ring-current criterion, probably peters out between [34] and [38]annulene.<sup>27</sup>

### 1.5.2 Antiaromatic Systems

A molecule with  $4n$   $\pi$  electrons in the ring, with the molecular orbitals made up from  $4n$  p orbitals, does not show this extra stabilisation. Molecules in this class that have been studied include cyclobutadiene **1.17**

( $n=1$ ), the cyclopentadienyl cation **1.18**, the cycloheptatrienyl anion **1.19**, cyclooctatetraene **1.20** and pentalene **1.21** ( $n=2$ ), [12]annulene **1.22** ( $n=3$ ) and [16]annulene **1.23** ( $n=4$ ).

We can see this most easily by looking at the molecular orbitals of square cyclobutadiene in Fig. 1.46. As usual, the lowest energy orbital  $\psi_1$  has no nodes, and, as with benzene and because of the symmetry, there are two exactly equivalent orbitals,  $\psi_2$  and  $\psi_3$ , with one node. The bonding in  $\psi_1$  is between atomic orbitals with coefficients of 0.500, not only between C-1 and C-2, but also between C-2 and C-3, between C-3 and C-4 and between C-4 and C-1. If the overlap in  $\psi_3$  of benzene, which also has coefficients of 0.500, gives an energy-lowering of  $1\beta$ , then the overlap in  $\psi_3$  of cyclobutadiene should give twice as much energy-lowering, since there are twice as many bonding interactions (this makes an assumption that the p orbitals are held at the same distance by the  $\sigma$  framework in both cases). In contrast, the bonding interactions both in  $\psi_2$  and  $\psi_3$  are exactly matched by the antibonding interactions, and there is no lowering of the energy below the line ( $\alpha$ ) representing the energy of a p atomic orbital on carbon. The molecular orbitals  $\psi_2$  and  $\psi_3$  are therefore nonbonding orbitals, and the net lowering in energy for the  $\pi$  bonding in cyclobutadiene is only  $2 \times 2\beta$ . The energies of the four  $\pi$  orbitals are again those we could have deduced from the model inscribing the conjugated system in a circle, with the point of the square at the bottom. The total  $\pi$  stabilisation of  $2 \times 2\beta$  is no better than having two isolated  $\pi$  bonds—there is therefore no special extra stabilisation from the cyclic conjugation relative to two isolated  $\pi$  bonds. There is however less stabilisation than that found in a pair of *conjugated* double bonds—the overall  $\pi$  bonding in butadiene, taking values from Fig. 1.40, is  $2 \times (1.618 + 0.618)\beta = 4.472\beta$  and the overall  $\pi$  bonding in cyclobutadiene is only  $2 \times 2\beta$  making it less stable by  $0.472\beta$ .

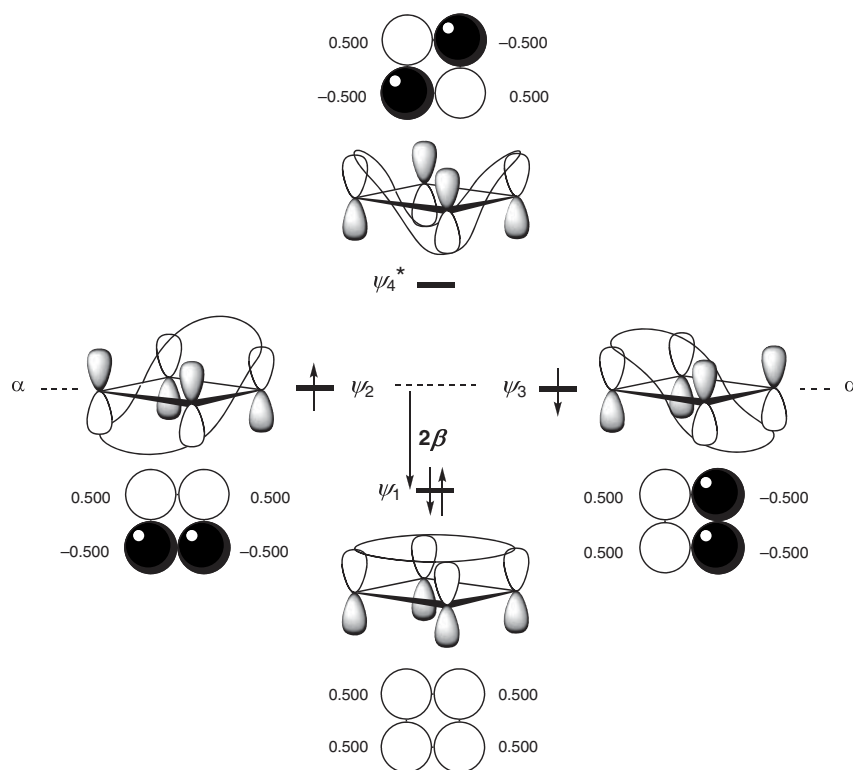
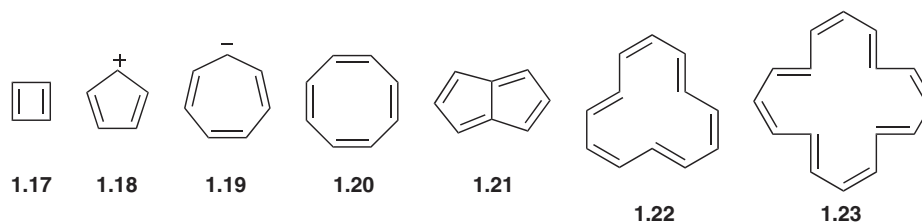
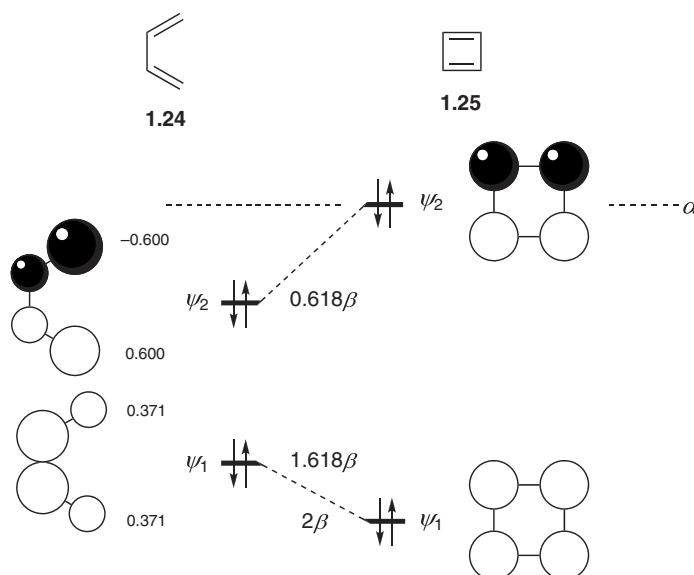


Fig. 1.46 The  $\pi$  molecular orbitals of cyclobutadiene



We can reach a similar conclusion from an interaction diagram, by looking at the effect of changing butadiene **1.24** into cyclobutadiene **1.25** (Fig. 1.47). This time there is one drop in  $\pi$  energy and one rise, and no net stabilisation from the cyclic conjugation. As with benzene, we can see that the drop is actually less (from overlap of orbitals with a small coefficient) than the rise (from overlap of orbitals with a large coefficient). Thus cyclobutadiene is less stabilised than butadiene.



**Fig. 1.47** No change in  $\pi$  energy in going from butadiene to cyclobutadiene

There is much evidence that cyclic conjugated systems of  $4n$  electrons show no special stability. Cyclobutadiene dimerises at extraordinarily low temperatures ( $>35\text{K}$ ).<sup>28</sup> Cyclooctatetraene is not planar, and behaves like an alkene and not at all like benzene.<sup>29</sup> When it is forced to be planar, as in pentalene, it becomes unstable to dimerisation even at  $0^\circ\text{C}$ .<sup>30</sup> [12]Annulene and [16]annulene are unstable with respect to electrocyclic reactions, which take place below  $0^\circ\text{C}$ .<sup>31</sup> In fact, all these systems appear on the whole to be significantly higher in energy and more reactive than might be expected, and there has been much speculation that they are not only lacking in extra stabilisation, but are actually destabilised. They have been called 'antiaromatic'<sup>32</sup> as distinct from nonaromatic. The problem with this concept is what to make the comparisons with. We can see from the arguments above that we can account for the destabilisation



relative to conjugated  $\pi$  bonds—linear conjugation is more energy-lowering than the cyclic conjugation of  $4n$  electrons, which goes some way to setting the concept of antiaromaticity on a physical basis. This argument applies to the thermodynamics of the system, which indirectly affects the reactivity. That  $4n$  systems are unusually reactive is also explicable with an argument based on the frontier orbitals, as we shall see later—the HOMO is unusually high in energy for a neutral molecule, at the nonbonding  $\alpha$  level for cyclobutadiene and the other uncharged cyclic hydrocarbons **1.18–1.23**, significantly above the level of the HOMO of the linear conjugated hydrocarbons, and at the same time the LUMO is correspondingly low in energy.

The prediction from the argument in Fig. 1.46 is that square cyclobutadiene ought to be a diradical with one electron in each of  $\psi_2$  and  $\psi_3$ , on the grounds that putting a second electron into an occupied orbital is not as energy-lowering as putting the first electron into that orbital (see Section 1.2). This is not borne out by experiment, which has shown that cyclobutadiene is rectangular with alternating double and single bonds and shows no electron spin resonance (ESR) signal.<sup>33</sup>

We can easily explain why the rectangular structure is lower in energy than the square. So far, we have made all  $\pi$  bonds contribute equally one  $\beta$ -value to every  $\pi$  bond. The difference in  $\beta$ -values, and hence in the strengths of  $\pi$  bonds, as a function of how closely the p orbitals are held, can be dealt with by defining a standard  $\beta_0$  value for a C=C double bond and applying a correction parameter  $k$ , just as we shall in Equation 1.16 for the effect of changing from a C=C double bond to a C=X double bond. Some values of  $k$  for different distances  $r$  can be seen in Table 1.1,<sup>34</sup> which was calculated with  $\beta_0$  based on an aromatic double bond, rather than the double bond of ethylene, and by assuming that  $\beta$  is proportional to the overlap integral  $S$ .

**Table 1.1** Variation of the correction factor  $k$  with distance  $r$

$r$ (Å)	$k$	$r$ (Å)	$k$
1.20	1.38	1.45	0.91
1.33	1.11	1.48	0.87
1.35	1.09	1.54	0.78
1.397	1.00		

In the rectangular structure of cyclobutadiene, the symmetry is lowered, and the molecular orbitals corresponding to  $\psi_2$  and  $\psi_3$  are no longer equal in energy (Fig. 1.48). The overall bonding in  $\psi_1$  is more or less the same as in the square structure—C-1 and C-2 (and C-3 and C-4) move closer together in  $\psi_1$ , and the level of bonding is actually increased by about as much as the level of bonding is decreased in moving the

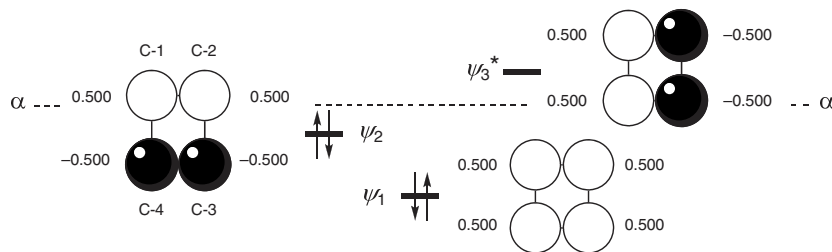


**Fig. 1.48** The three lowest-energy  $\pi$  molecular orbitals of rectangular cyclobutadiene

other pairs apart. In the other filled orbital,  $\psi_2$ , the same distortion, separating the pair (C-1 from C-4 and C-2 from C-3) will reduce the amount of  $\pi$  antibonding between them, and hence lower the energy. The corresponding argument on  $\psi_3$  will lead to its being raised in energy, and becoming an antibonding orbital. With one  $\pi$  orbital raised in energy and the other lowered, the overall  $\pi$  energy will be much the same, and the four electrons then go into the two bonding orbitals. This is known as a Jahn-Teller distortion, and can be expected to be a factor whenever a HOMO and a LUMO are very close in energy,<sup>35</sup> as we have already seen with very long conjugated systems in Section 1.4.3. The square structure will be the transition structure for the interconversion of the one rectangular form into the other, a reaction that can be expected to be fairly easy, but to have a discernible energy barrier. Proper molecular orbital calculations support this conclusion.<sup>36</sup> We must be careful in arguments like this, based only on the  $\pi$  system, not to get too carried away. We have not allowed for distortions in the  $\sigma$  framework in going from the square to the rectangular structure, and this can have a substantial effect.

### 1.5.3 The Cyclopentadienyl Anion and Cation

A slightly different case is provided by the cyclopentadienyl anion and cation. The device of inscribing the pentagon in a circle sets up the molecular orbitals in Fig. 1.49. The total of  $\pi$  bonding energy is  $2 \times 3.236\beta = 6.472\beta$  for the anion, in which there are two electrons in  $\psi_1$ , two electrons in  $\psi_2$ , and two electrons in  $\psi_3$ . The anion is clearly aromatic, since the open-chain analogue, the pentadienyl anion has only  $2 \times 2.732\beta = 5.464\beta$  worth of  $\pi$  bonding (Fig. 1.40), the extra stabilisation being close to  $1\beta$ , and closely similar to the extent by which benzene is lower in energy than its open-chain analogue, hexatriene. The cyclopentadienyl anion **1.11**, a  $4n+2$  system, is well known to be exceptionally stabilised, with the  $pK_a$  of cyclopentadiene at 16 being strikingly low for a hydrocarbon. The cation, however, has  $\pi$ -bonding energy of  $2 \times 2.618\beta = 5.236\beta$ , whereas its open-chain analogue, the pentadienyl cation, in which there are two electrons in  $\psi_1$  and two electrons in  $\psi_2$ , has more  $\pi$  bonding, specifically  $2 \times 2.732\beta = 5.464\beta$ . The cyclopentadienyl cation **1.18**, a  $4n$  system, can be expected to be thermodynamically high in energy overall and therefore difficult to make, and so it is known to be. The cyclopentadienyl cation is not formed from its iodide by solvolysis under conditions where even the unconjugated cyclopentyl iodide ionises easily.<sup>37</sup> In addition, the cyclopentadienyl cation ought to be especially electrophilic for kinetic reasons, since the energy of the LUMO is actually below the  $\alpha$  level. It is also known to be a diradical in the ground state.<sup>38</sup> The fluorenyl cation, the dibenz analogue of the cyclopentadienyl cation, however, does not appear to be significantly higher in energy than might be expected of a doubly benzylic cation held coplanar.<sup>39</sup>

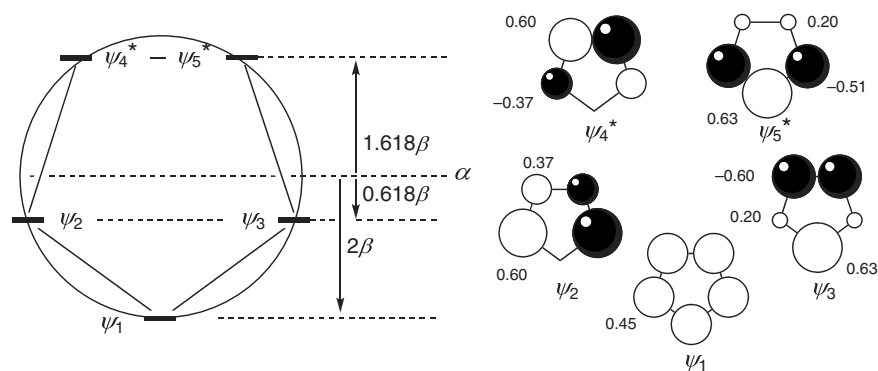


Fig. 1.49 The energies and coefficients of the  $\pi$  molecular orbitals of the cyclopentadienyl system

A striking difference between all the aromatic and all the antiaromatic systems is the energy *difference* between the HOMO and the LUMO. The aromatic systems have a substantial gap between the frontier orbitals, and the antiaromatic systems a zero gap in simple Hückel theory or a small gap if the Jahn-Teller distortion is allowed for. The difference in energy between the HOMO and the LUMO correlates with the hardness of these hydrocarbons as nucleophiles, and with some measures of aromaticity.<sup>40</sup> For example, in antiaromatic rings with  $4n$  electrons, there is a paramagnetic ring current, which is a manifestation of orbital effects, just like the diamagnetic ring currents from aromatic rings. The protons at the perimeter of a  $4n$  annulene, when it is stable enough for measurements to be made, are at high field, and protons on the inside of the ring are at low field. The slow interconversion of the double and single bonds in antiaromatic systems means that there is no free movement of the electrons round the ring, and so any diamagnetic anisotropy is muted. At the same time, the near degeneracy of the HOMO and the LUMO in the  $4n$  annulenes allows a low-energy one-electron transition between them with a magnetic moment perpendicular to the ring, whereas the aromatic systems, with a much larger energy gap between the highest filled and lowest unfilled orbitals do not have this pathway.<sup>41</sup> Single electrons are associated with induced paramagnetic fields, as seen in the ESR spectra of odd electron systems.

#### 1.5.4 Homoaromaticity<sup>42</sup>

The concept of aromaticity can be extended to systems in which the conjugated system is interrupted, by a methylene group, or other insulating structural feature, provided that the overlap between the p orbitals of the conjugated systems can still take place through space across the interruption. When such overlap has energy-lowering consequences, evident in the properties of the molecule, the phenomenon is called homoaromaticity. Examples are the homocyclopropenyl cation **1.26**, the trishomocyclopropenyl cation **1.27**, the bishomocyclopentadienyl anion **1.28** and the homocycloheptatrienyl cation **1.29**. Each of these species shows evidence of transannular overlap, illustrated, and emphasised with a bold line on the orbitals, in the drawings **1.26b**, **1.27b**, **1.28b** and **1.29b**. The same species can be drawn without orbitals in localised structures **1.26a**, **1.27a**, **1.28a** and **1.29a** and with the drawings **1.26c**, **1.27c**, **1.28c** and **1.29c** showing the delocalisation. For simplicity, the orbital drawings do not illustrate the whole set of  $\pi$  molecular orbitals, which simply resemble in each case the  $\pi$  orbitals of the corresponding aromatic system.

However, homoaromaticity appears to be absent in homobenzene (cycloheptatriene) **1.30a** and in trishomobenzene (triquinacene) **1.31a**, even though transannular overlap looks feasible. In both cases, the conventional structures **1.30a** and **1.30c**, and **1.31a** and **1.31c** are lower in energy than the homoaromatic structures **1.30b** and **1.31b**, which appear to be close to the transition structures for the interconversion.

